Developmental Biology 391 (2014) 17–31

Contents lists available at ScienceDirect

Developmental Biology

journal homepage: www.elsevier.com/locate/developmentalbiology

# *Tbx18* is essential for normal development of vasculature network and glomerular mesangium in the mammalian kidney

Jinshu Xu [a,1], Xuguang Nie [a,1,2], Xiaoqiang Cai [b,c,d], Chen-Leng Cai [b,c,d], Pin-Xian Xu [a,b,*]

[a] Department of Genetics and Genomic Sciences, Icahn School of Medicine at Mount Sinai, New York, NY 10029, USA
[b] Department of Developmental Biology and Regenerative Medicine, Icahn School of Medicine at Mount Sinai, New York, NY 10029, USA
[c] Center for Molecular Cardiology, Icahn School of Medicine at Mount Sinai, New York, NY 10029, USA
[d] Black Family Stem Cell Institute, Icahn School of Medicine at Mount Sinai, New York, NY 10029, USA

ARTICLE INFO

*Article history:*
Received 7 October 2013
Received in revised form
11 March 2014
Accepted 6 April 2014
Available online 12 April 2014

*Keywords:*
*Tbx18*
Kidney
Stromal cell
Interstitium
Perivascular mesenchyme
Glomerular mesangium
Vasculogenesis

ABSTRACT

*Tbx18* has been shown to be essential for ureteral development. However, it remains unclear whether it plays a direct role in kidney development. Here we addressed this by focusing on examining the pattern and contribution of *Tbx18*+ cells in the kidney and its role in kidney vascular development. Expression studies and genetic lineage tracing revealed that *Tbx18* is expressed in renal capsule, vascular smooth muscle cells and pericytes and glomerular mesangial cells in the kidney and that *Tbx18*-expressing progenitors contribute to these cell types. Examination of $Tbx18^{-/-}$ kidneys revealed large reduction in vasculature density and dilation of glomerular capillary loops. While SMA+ cells were reduced in the mutant, PDGFRβ+ cells were seen in early capillary loop renal corpuscles in the mutant, but fewer than in the controls, and further development of the mesangium failed. Analysis of kidney explants cultured from E12.5 excluded the possibility that the defects observed in the mutant were caused by ureter obstruction. Reduced proliferation in glomerular tuft and increased apoptosis in perivascular mesenchyme were observed in $Tbx18^{-/-}$ kidneys. Thus, our analyses have identified a novel role of *Tbx18* in kidney vasculature development.



## Introduction

The mammalian metanephric kidney development is initiated via inductive interactions between the metanephric mesenchyme (MM) and ureteric bud (UB) (Saxen and Sariola, 1987; Saxen et al., 1986), both derived from intermediate mesoderm. The MM contains precursors of distinct cell lineages, including nephrogenic and stromal precursors (Dressler, 2006). Nephrogenic progenitors condense around the nascent UB tips to form cap mesenchyme, which secretes inductive signaling molecules to induce UB branching. The cap mesenchymal cells are not only induced to form nephron tubules via mesenchymal–epithelial transformation but a subpopulation of the cells is selected for self-renewal to support continuous UB branching morphogenesis to generate certain number of nephrons. The stromal cells, initially formed at the periphery of the MM, migrate within the developing kidney and form renal interstitium and a set of important supporting tissues by differentiating into fibroblasts, vascular smooth muscle cells (SMCs) and pericytes (Alcorn et al., 1999; Cullen-McEwen et al., 2005; Dressler, 2006; Oliver et al., 2002; Sequeira Lopez and Gomez, 2011). Previous studies have provided direct evidence that renal stromal or interstitial cells are required for renal epithelial morphogenesis and disruption of stromal cell development severely perturbs nephron differentiation and collecting system morphogenesis (Batourina et al., 2001; Hatini et al., 1996; Mendelsohn et al., 1999; Quaggin et al., 1999; Saxen and Sariola, 1987).

While the UB undergoes repetitive branching morphogenesis to generate collecting system and the cap mesenchymal progenitors go through a series of well-characterized morphologically different comma-, S-shaped body and capillary loop stages to generate mature nephron, a third important component of the kidney, the vasculature, is formed simultaneously through both in situ vascularization and extrinsic vessel invasion (angiogenesis) (Abrahamson et al., 1998; Del Porto et al., 1999; Gomez et al., 1997; Oliver and Al-Awqati, 2000; Oliver et al., 2002; Risau and Ekblom, 1986; Risau et al., 1988). Major vessels of kidneys are likely formed through budding from existing vessels (descending aorta and concomitant vein). These new vessels invade into the renal blastema and interconnect with developing vascular network to form the renal vasculature (Del Porto et al., 1999; Gomez et al., 1997; Oliver and

* Corresponding author at: Department of Genetics and Genomic Sciences, Mount Sinai School of Medicine, New York, NY 10029, USA.
*E-mail address:* pinxian.xu@mssm.edu (P.-X. Xu).
[1] Authors contributed equally to this work.
[2] Present address: Department of Pathology, Johns Hopkins Hospital, Johns Hopkins University, Baltimore, MD 21205, USA.

http://dx.doi.org/10.1016/j.ydbio.2014.04.006
0012-1606/

Al-Awqati, 2000; Oliver et al., 2002; Risau and Ekblom, 1986; Risau et al., 1988). Current evidence indicates that angiogenic cells within the renal blastema are likely derived from hemangioblast cells, whereas their associated mesenchymal cells are derived from stromal cells (Faa et al., 2012; Sequeira Lopez and Gomez, 2011). The vasculature in the glomerulus consists of capillary loops and associated mesangial cells. The capillary loop enters into the proximal epithelial cleft formed in the S-shaped stage of the developing nephron and branches to produce the complex capillary tuft, while mesangial cells populate the core of the tuft and connect the capillary loops through the deposition of mesangial matrix, which becomes focally attached to the glomerular basement membrane produced by the podocytes and endothelial cells (Dressler, 2006). Development of the renal vasculature is highly interrelated with nephrogenesis to form an efficient filtration system (Kloth et al., 1994).

The T-box family transcription factor Tbx18 is essential for normal development of a variety of tissues and organs (Airik et al., 2006; Bussen et al., 2004; Cai et al., 2008; Farin et al., 2008). Published studies on *Tbx18* function in renal development have focused on the ureter. *Tbx18* is strongly expressed in the ureteral mesenchyme and is essential for the development of ureteral SMCs (Airik et al., 2006; Nie et al.). Loss of *Tbx18* in mice leads to hydroureter and hydronephorosis due to abnormal development of the ureter SMCs (Airik et al., 2006). $Tbx18^{-/-}$ mice also showed kidney dismorphogenesis and cystic dilation, which were suggested to be secondary to hydroureter and hydronepherosis (Airik et al., 2006). A most recent study reported that *Tbx18*+ cells contribute to multipotent precursor population in the developing urogenital system, including mesenchymal cell populations in the kidney (Bohnenpoll et al., 2013). However, it remains unclear whether *Tbx18* is expressed in the kidney and whether it has a primary role during kidney development. To begin to address if *Tbx18* plays a role during kidney development, here we analyzed pattern and contribution of *Tbx18*-expressing cells in the kidney and examined *Tbx18*-deficient kidneys at earlier stages before the onset of ureteric obstruction as well as in kidney explant culture. Our data indicate that *Tbx18* is expressed in renal stromal cell-derived vascular SMCs and pericytes and glomerular mesangial cells and that the development of vasculature network and glomerular tuft depends on *Tbx18* function, revealing a previously unidentified role of *Tbx18* in kidney vasculature development.

## Material and methods

### Mice

$Tbx18^{LacZ/+}$ ($Tbx1^{+/-}$), $R26R^{LacZ}$ and *Hoxb7-Egfp* mice were described previously (Cai et al., 2008; Soriano, 1999; Srinivas et al., 1999; Xu et al., 2003). In the $Tbx18^{Cre}$ line, the neocassette was removed by crossing with the flippase mice (Jackson Laboratory, 007844), which was not removed in the previously published $Tbx18^{Cre}$ line (Cai et al., 2008). The compound mutants carrying the *Hoxb7-GFP* transgene (Srinivas et al., 1999) in a mixed C57BL6/CBA/129 background to mark the ureteric epithelium were used for analysis. All procedures involving living mice were approved by the Animal Care and Use Committee at the Mount Sinai School of Medicine.

### Ink injection for renal vessels

Ink was injected through renal vein with a constant pressure as described previously (Moffat and Fourman, 2001). Injected kidneys were dehydrated and visualized in solution of benzyl alcohol and benzyl benzoate (1:1).

### Dissection of arterial trees

Kidneys were collected and microdissected as described previously (Casellas et al., 1993). Briefly, the kidneys were incubated in 6 M hydrochloric acid for 30 min at 42 °C, and then washed several times with acidified water (pH 2.5). The entire intrarenal arterial vasculature (arterial tree) was then carefully dissected from each kidney.

### Histology and X-gal staining

Dissected kidneys were fixed in 4% paraformaldehyde (PFA) for 1 h and processed for histological analysis following standard procedure. Frontal section was used for kidney examination unless otherwise described.

X-gal was performed as described (Xu et al., 2003). Whole-mount kidneys were fixed in 4% PFA for 15 min at 4 °C and stained at 37 °C overnight for embryonic samples or at 4 °C for 2–3 days for neonate samples. Cryosections were generated at 10–12 μm using a Microm HM 550 cryostat and stained with X-gal at 37 °C overnight to 24 h and counterstained with diluted hematoxylin.

### Immunohistochemistry and in situ hybridization

Anti-β-gal (Abcam, ab9361), -α-SMA (Sigma, clone 1A4 and A5228), -smooth muscle heavy chain (SMHC) (Thermo, clone SM-M10ik), -fibronectin (Sigma, clone FN-3E2), -PDGFRβ (Santa Cruz, sc1627), -WT1 (Santa Cruz, sc192), -PECAM-1 (Santa Cruz, sc376764), and -cytokeratin (Abcam, ab9217), and SIX2 (Santa Cruz, sc377193) antibodies were used for immunodetection on sections. Secondary antibodies were either peroxidase- or Cy3- or fluorescein-conjugated. DAB was used for peroxidase mediated color reaction. AP-conjugated α-SMA (Sigma, clone1A4) antibody was used for whole mount staining.

Section in situ hybridization was carried out with digoxigenin-labeled riboprobes specific for *Wt1*, *Tbx18* and *SM22* (Nie et al., 2010).

### Organ cultures

E12.5 kidneys with ureters attached were cultured in medium as described previously (Bohnenpoll et al., 2013). The culture medium was replaced every 24 h and images were taken every 24 h. After 4 days in culture, explants were fixed and processed for histology and immunostaining.

### Proliferation and apoptosis assay

Anti-PCNA (clone PC10, Pierce) was used to label proliferative cells at S-phase and anti-γH2AX antibody (Santa Cruz, SC-101696) was used for detecting DNA double-strand breaks. TUNEL assay for apoptosis and BrdU labeling for proliferation assay were also performed as previously described (Nie et al.). The number of proliferating cells was counted in serial sections from each glomerulus, and at least 30 glomeruli of each genotype were counted.

## Results

### *Tbx18 is expressed in renal capsule, vascular SMCs and pericytes and glomerular mesangial cells in the kidney*

To test if *Tbx18* has a direct role in kidney vasculature development, we first investigated its expression during kidney development by performing X-gal staining for the $Tbx18^{LacZ}$ knockin

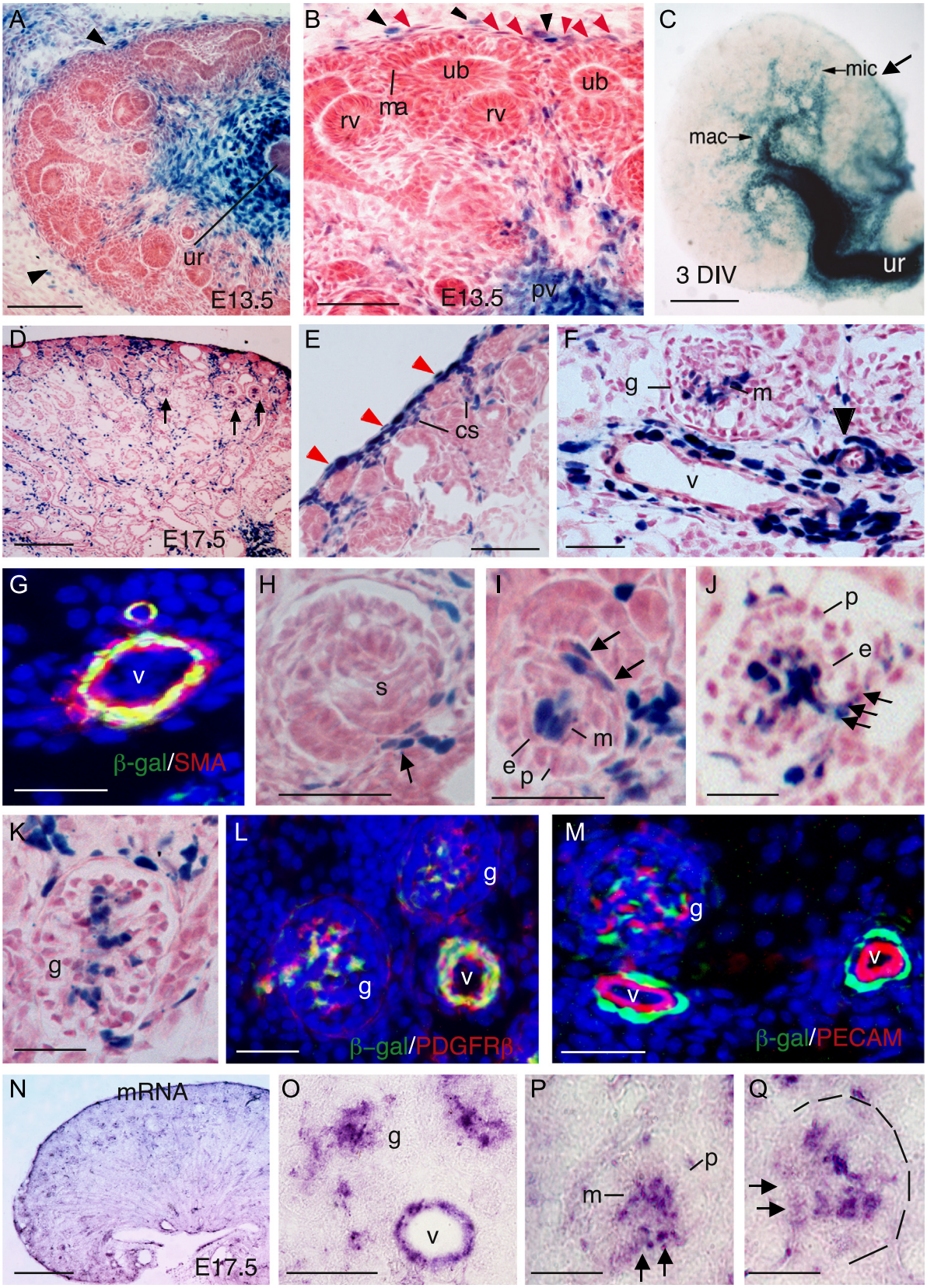


**Fig. 1.** *Tbx18* expression in developing kidney. (A) X-gal stained sections of $Tbx18^{lacZ/+}$ kidney at E13.5. (B) Higher magnification of panel A. Lack arrowheads point to LacZ+ cells in the renal capsule and red arrowheads point to weak lacZ+ stromal cells. (C) Whole-mount X-gal stained rudiment after 3 days in vitro (DIV) of E12.5 kidney. Arrow points to strong *LacZ* expression in the capsule. (D) X-gal stained sections of $Tbx18^{lacZ/+}$ kidney at E17.5. Arrows point to developing glomeruli. (E and F) Higher magnification of panel D. Red arrowheads in (E) point to LacZ+ renal capsule cells and black arrowhead in (F) points to small vessel. (G) Immunostaining of E17.5 kidney section showing *Tbx18*+ (β-gal+)/SMA+ perivascular cells. (H) Higher magnification showing *Tbx18* expression in cells associated with the capillary sprout entering into the S-shaped glomerulus (s) (arrow). (I) Early stage, (J) late stage, and (K) more mature glomeruli labeled for *Tbx18*. Note that the mesangial core (m) is strongly labeled and that this labeling is continuous with afferent and efferent arteriolar walls (arrows). Note that the podocytic (p) and endothelial (e) layers lack *Tbx18* expression. (L and M) Co-immunostaining showing that *Tbx18*+ cells in vasculature and glomerulus (g) are PDGFRβ+ (L) but PECAM- (M). (N–Q) Section in situ hybridization using dig-labeled *Tbx18* riboprobe showing *Tbx18* mRNA expression in vascular mesenchyme (v) and mesangial core (m) as well as in continuous with afferent and efferent arteriolar walls (arrows). Other abb.: mac, major calyces; ma, mesenchymal aggregate; pv, pelvis; rv, renal vesicle; ub, ureteric bud; ur, ureter; v, vessels. Scale bar: 200 μm for A, D, and N, 100 μm for B, E, and F, 400 μm for C, and 25 μm for E–M and O–Q.

reporter. As expected, X-gal staining of kidney sections revealed strong *Tbx18* expression in the ureteral mesenchyme and its extended mesenchyme surrounding the renal pelvis, papilla and calyces at E13.5–17.5 (Fig. 1A–C and data not shown). At E13.5, strong *Tbx18* expression was observed in the renal capsule, whereas its expression in cortical stromal cells was relatively weak (Fig. 1A and B). In the developing renal capsule, its expression was first seen in the ventral side of the capsular stroma close to the ureter (arrow, Fig. 3C). At E15.5–17.5, *Tbx18*+ cells were detected in the renal capsule and a proportion of the mesenchymal cells in the developing renal cortex and medulla (Fig. 1D and E). The *Tbx18*+ cells in the cortex were located in the vicinity of developing interlobular arteries and afferent or efferent glomerular arterioles and stromal cells (Fig. 1D and F). *Tbx18*+ cells were also detected in glomeruli (Fig. 1D and F). The periendothelial mural pericytes (arrowhead, Fig. 1F) and smooth muscle cells (SMCs) (larger vessels) were *Tbx18*+ cells (Fig. 1F), which were marked by α-smooth muscle actin (SMA) (Fig. 1G) or PDGFRβ (Fig. 1L). SMA is a marker for a more differentiated population of SMCs and pericytes (Lindahl et al., 1998), while PDGFRβ marks precursors of vascular SMCs and pericytes and mesangial cells in the glomerulus (Lindahl et al., 1997, 1998).

In the developing glomerulus, *Tbx18* was first seen in singular cells associated with the growing capillary loop in the S-shaped stage of glomerular development (Fig. 1H). Groups of *Tbx18*+ cells collected at the base and in the mesenchymal core of capillary loop renal corpuscle (Fig. 1I and J). In the more mature glomerular tufts, the *Tbx18*+ cells were clearly confined to the mesangial cells of the tuft that are positive for PDGFRβ (Fig. 1K and L). No β-gal activity was observed in the cap mesenchyme and epithelial or endothelial structures at all stages examined (Fig. 1A–M). In situ hybridization using digoxigenin-labeled *Tbx18* riboprobe confirmed endogenous *Tbx18* mRNA expression in the cell types that were positive for the $Tbx18^{LacZ}$ reporter (Fig. 1N–Q). Thus, our data demonstrate that *Tbx18* is expressed in the developing renal capsule, vascular SMCs and pericytes and glomerulus mesangial cells, suggesting that *Tbx18* may have a direct role in regulating the development of these cell types in the kidney.

### *Lineage tracing analysis reveals contribution of Tbx18-derived progenitors to renal capsule, vasculature and interstitium*

To better understand the involvement of *Tbx18* in kidney development, we further investigated the cell lineages derived from *Tbx18*-expressing progenitors by performing a lineage tracing analysis using *Tbx18-Cre* knock-in mice and the lineage reporter $R26R^{LacZ}$ mice (Soriano, 1999) to permanently label descendants from the *Tbx18*+ cells. Analysis of *lacZ* expression on sections of $Tbx18^{Cre/+}$;$R26R^{LacZ}$ kidneys derived from the cross between $Tbx18^{Cre}$ and $R26R^{LacZ}$ revealed strong β-gal activity in subpopulations of mesenchymal cells at E17.5 (Fig. 2B). No β-gal activity was observed in $Tbx18^{Cre/+}$ or $R26R^{LacZ}$ controls (Fig. 2A and data not shown).

Similar to the active *Tbx18* expression, in addition to the ureteral mesenchyme and its extended mesenchyme in the pelvis, papilla and calyces, strong β-gal activity was detected in subpopulation of cells in the capsule, cortex and medulla of the kidney. X-gal or anti-β-gal staining and marker analysis confirmed that vascular mesenchymal SMCs and pericytes and glomerular mesangial cells were descendants of *Tbx18*+ cells (Fig. 2C–K). In contrast, the endothelial cells marked by PECAM (Fig. 2L) and the MM-derived cells podocytes marked by WT1 were β-gal− (Fig. 2M), confirming that these cells are not linearly related to *Tbx18*+ cells. In addition, no β-gal+ cells were detected at the collecting duct marked by cytokeratin (data not shown), confirming that the *Tbx18*+ progenitors do not contribute to the ureteric tip. Together, these data demonstrate that *Tbx18*-derived cells give rise to multiple mesenchymal cell types that originate from stromal cells in the kidney, including perivascular mesenchymal cells and glomerular mesangial cells.

X-gal staining of kidneys from adult $Tbx8^{Cre/+}$;$R26R^{LacZ}$ mice revealed LacZ+ cells in the capsule, mesangium of glomeruli, interstitium and papilla (Fig. 3A–C). Vascular SMA+ smooth muscle was β-gal+ (Fig. 3D) and SMA+ SMCs in the pelvic region were also β-gal+ (data not shown), while only very few β-gal+ cells in the interstitium were SMA+ (arrowhead, Fig. 3D and F). In contrast, almost all β-gal+ cells in the interstitium were PDGFRβ+ (Fig. 3E and F), identifying them as pericytes/perivascular fibroblasts. All β-gal+ cells in the renal capsule were also PDGFRβ+ (Fig. 3G). No contribution was seen to other structures of the kidney, suggesting that there is no ongoing recruitment of this mesenchymal population to ureteric or tubular epithelia.

Our results indicate that *Tbx18*+ cells are stromal cells, which originate from *Foxd1*+ progenitors. However, unlike strong *Foxd1* expression in the mesenchyme dorsal to the MM at E11.5 (Bohnenpoll et al., 2013; Hatini et al., 1996), *Tbx18* is strongly expressed in the mesenchyme ventral to the metanephric region at E11.5 (Fig. S1A and B) (Airik et al., 2006; Bohnenpoll et al., 2013; Nie et al.) and its expression was almost undetectable in the cortical stroma at E12.5 (Fig. S1C). A recent study suggested that a *Tbx18*-expressing mesenchymal population dorsal to the MM within the metanephric region at E10.5 might be detectable by whole-mount in situ hybridization and might overlap with *Foxd1*+ progenitors (Bohnenpoll et al., 2013). To clarify this, we performed lineage tracing at E11.5–12.5 before *Tbx18* becomes actively expressed in the kidney cortical stroma. X-gal staining of kidney sections from $Tbx18^{Cre/+}$;$R26R^{LacZ/+}$ embryos barely detected *Tbx18*+ lineage in the stromal mesenchyme dorsal to the MM at E11.5 (Fig. S1E and F) and the cortical stroma at E12.5 (Fig. S1G and H), differing from the pattern of *Foxd1* expression at these stages (Bohnenpoll et al., 2013; Hatini et al., 1996). Instead, lineage tracing at these stages revealed *Tbx18*+ lineage in the ureteral mesenchyme, its extended mesenchyme in the cylaces and pelvis and renal capsule, a pattern similar to its active expression labeled by *Tbx18* riboprobe or $Tbx18^{LacZ}$ (Fig. S1A–C). In contrast to the wide distribution of *Tbx18*-derived cells in the mesenchyme ventral to the kidney at E12.5 (Fig. S1G and H), *Tbx18* expression in the ventral mesenchyme became more restricted to the ureteral mesenchyme (Fig. S1C). In the renal capsule, comparing to its active expression (Fig. S1C), more *Tbx18*+ descendants were observed (Fig. S1G and H). This could be due to the difference between the expression levels of the *Tbx18-LacZ* and the *R26R-LacZ* reporters. Nonetheless, our results suggest that $Tbx18^{Cre}$ is not active in the cortical stromal progenitors before E12.5 and that strong *Tbx18* expression in the cortical stroma is likely induced after E12.5.

### *Abnormal development of renal vasculature network in $Tbx18^{-/-}$ mice*

To examine whether *Tbx18* plays a role during kidney development, we performed a detailed analysis of wild-type control, $Tbx18^{+/-}$ and $Tbx18^{-/-}$ kidneys at different developmental stages. While $Tbx18^{+/-}$ kidneys appeared normal when compared to wild-type controls (Fig. 4A and data not shown), kidneys of $Tbx18^{-/-}$ embryos failed to ascend but were rotated 90° downward, becoming flat with front-facing pelvis in the caudal portion (Fig. 4B). The genital organs (ovary and testis) also failed to descend properly (Fig. 4B). Histological analysis at E18.5 revealed cyst formation and dilation of epithelial structures of the nephrons and collecting system in $Tbx18^{-/-}$ kidneys (data not shown), which were previously suggested to be secondary defects caused

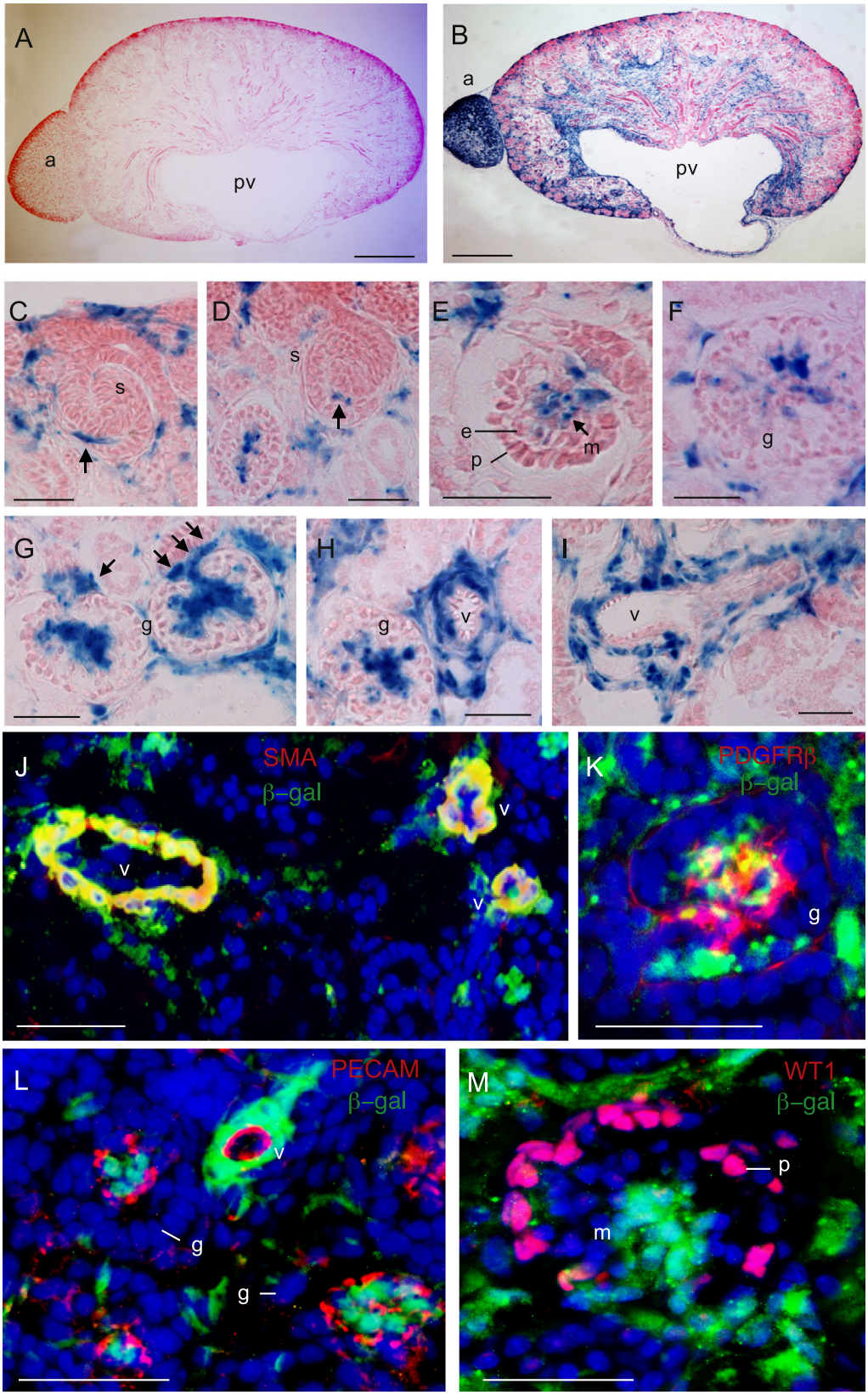


**Fig. 2.** Contribution of *Tbx18*-derived progenitors to renal vascular system and interstitium. (A and B) X-gal staining on kidney sections of $R26R^{LacZ}$ (A) or $Tbx18^{Cre}$;$R26R^{lacZ}$ (B) embryos at E17.5. (C and D) Higher magnification of X-gal stained sections from $Tbx18^{Cre}$;$R26R^{lacZ}$ embryos at E17.5 showing *Tbx18*-derived cells are associated with the capillary sprout entering into the S-shaped glomerulus (s) (arrows). (E) Early, (F) mature and (G) late cup-shaped glomerular mesangial cells are derived from *Tbx18*+ cells but podocytes and endothelial cells are not linearly related to *Tbx18*+ cells. (H and I) Perivascular mesenchyme is originated from *Tbx18*+ cells. (J) Co-immunostaining with β-gal and α-SMA antibodies showing that vascular α-SMA+ cells are vascular β-gal+ (arrows). (K) Co-immunostaining with β-gal and PDGFRβ antibodies showing glomerular mesangial cells double positive for β -gal and PDGFRβ (arrows). (L and M) Co-immunostaining with β-gal along with PECAM-1 and WT1 antibodies showing no β-gal+ cells are positive these two markers glomeruli (g) and vessels. Other abb.: g, m, mesangial cells; v, vessels. Scale bar: 200 μm for A and B, and 50 μm for C–M.

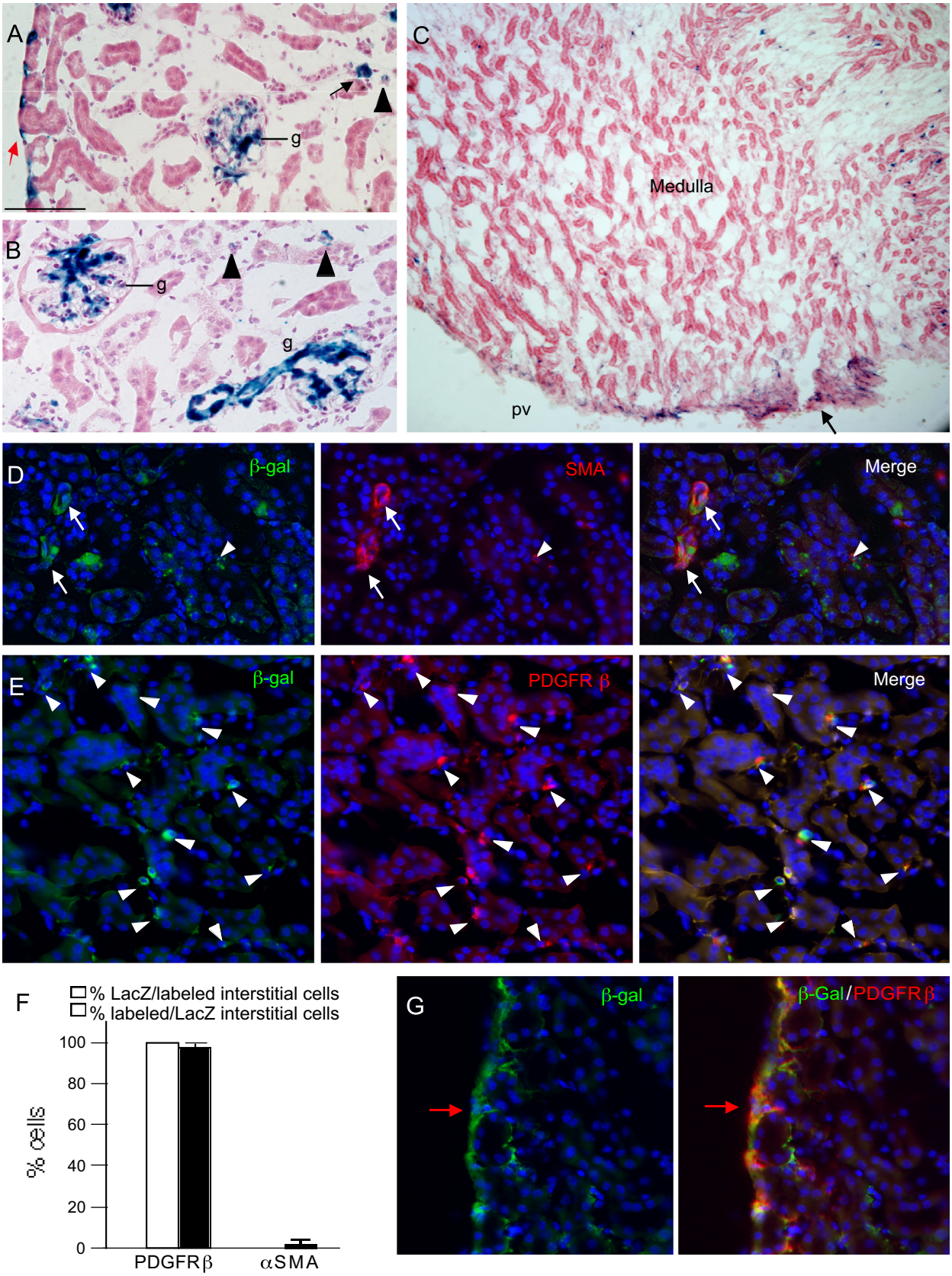


**Fig. 3.** Characterization of *Tbx18*+ cells in the adult kidney of *Tbx18*$^{Cre/+}$;*R26R*$^{LacZ/+}$ mice. (A and B) X-gal stained kidney sections showing LacZ+ cells in renal capsule (red arrow), glomeruli (g), vessels (black arrows), interstitium (arrowheads). (C) X-gal stained kidney section showing LacZ+ cells in the medullary region and renal papilla (arrow). (D) Kidney sections co-stained with anti-β-gal and -αSMA antibodies showing perivascular cells double positive for αSMA and β-gal (arrows). Arrowhead points to double positive cell in interstitium. (E) Kidneys sections co-stained with anti-β-gal and -PDGFRβ showing double positive cells in the interstitium (arrowheads). (F) Graph showing quantification of the proportion of PDGFRβ+ or αSMA+ interstitial cells co-expressing β-gal and the proportion of β-gal+ interstitial cells co-expressing PDGFRβ. (G) Kidney sections co-stained with anti-β-gal and -PDGFRβ showing double positive cells in the renal capsule (red arrow). Scale bar: 100 μm for A and B, 200 μm for C and 50 μm for D, E, and G.

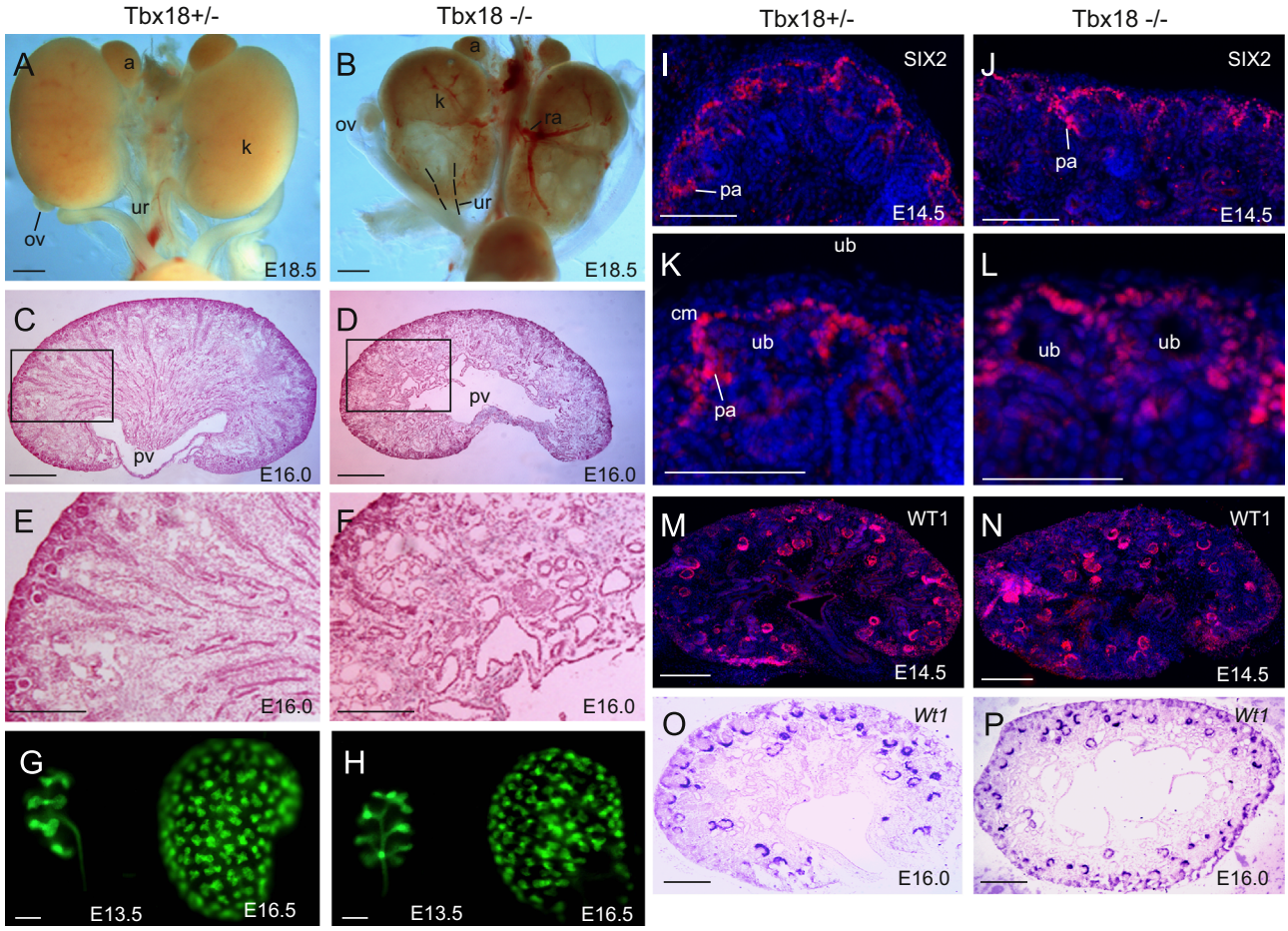


**Fig. 4.** Abnormal kidney development in *Tbx18*$^{-/-}$ mice. (A and B) Gross appearances of *Tbx18*$^{+/-}$and *Tbx18*$^{-/-}$ mutant littermate kidneys at E18.5. (C and D) Histology of *Tbx18*$^{+/-}$ and *Tbx18*$^{-/-}$ kidneys at E16.0. (E and F) Higher magnification of boxed areas in C and D. (G and H) *Hoxb7-GFP* tracing ureteric epithelial branching morphogenesis in *Tbx18*$^{+/-}$ and *Tbx18*$^{-/-}$ mutant at E13.5 and E16.5. (I and J) Immunostaining showing SIX2 expression in the metaneprhic mesenchymal progenitors at E14.5 in *Tbx18*$^{+/-}$ and *Tbx18*$^{-/-}$ kidneys. No noticeable difference in the levels of SIX2 was observed between *Tbx18*$^{+/-}$ and *Tbx18*$^{-/-}$ kidneys. (K and L) Higher magnification of panels I and J. (M and N) Immunostaining for WT1 on kidney sections from *Tbx18*$^{+/-}$ and *Tbx18*$^{-/-}$ embryos at E14.5. (O and P) Section in situ showing *Wt1* expression in *Tbx18*$^{+/-}$ and *Tbx18*$^{-/-}$ kidneys at E16.0. Note due to defects in UB branching and nephrogenesis, on some sections, *Wt1*-labeled developing nephrons were more than those in controls. Abb.: k, kidney; ov, ovary; pv, pelvis; ub, ureteric ud; ur, ureter. Scale bar: 50 μm for A–D, G, and H and 25 μm for E, F, and I–P.

by hydroureter and hydronephrosis due to abnormal development of ureteral SMCs (Airik et al., 2006). However, these defects were observed at ~E16.0 (Fig. 4C–F), slightly earlier than the onset of ureter dilation, which occurs from ~E16.5 (Airik et al., 2006), suggesting that the epithelial dilation/cystogenesis could be a primary defect that occurs in *Tbx18*$^{-/-}$ kidneys.

Ureteric epithelial tracing of *Hoxb7-GFP* of *Tbx18*$^{-/-}$ kidneys from earlier stages revealed that the pattern of collecting system arborization was altered in the mutant due to malpositioning of the pelvic region. The UB branches anterior–posterior symmetrically to form the first "T-bud" within the MM located lateral to the ureter (Fig. 4G), whereas it occurred left–right symmetrically in *Tbx18*$^{-/-}$ kidneys (Fig. 4H). Between E11.5 and 13.5, the rate of branching appeared normal in the mutant. By E16.5, we found that the tip number in the mutant was decreased by 9–15% when compared to the *Tbx18*$^{+/-}$ littermates (data not shown), suggesting that the number of branching events in the homozygous mutant was reduced. Molecular marker analysis revealed that the neprhogenic mesenchyme of the *Tbx18*$^{-/-}$ kidneys was able to condense and form pre-nephrogenic structures as labeled by SIX2 (Fig. 4I–L), a marker for undifferentiated MM and pre-tubular aggregates. The subsequent mesenchyme-to-epithelium transformation was not blocked in the *Tbx18*$^{-/-}$ kidneys as labeled with WT1 antibody (Fig. 4M and N) or *Wt1* riboprobe between E13.5 and 16.0 (Fig. 4O and P and data not shown). The *Tbx18*$^{-/-}$ kidneys also displayed lectin+ tubules in the cortex and juxtamedullary region of the kidney at E16.0–18.5 (data not shown), suggesting that nephron differentiation was not blocked in the mutant. Together, our data suggest that although initiation of branching and nephron differentiation occurs in the mutant, the branching rate is reduced in the mutant.

Interestingly, careful examination of histological sections revealed dilation of capillaries in maturing glomeruli at E15.5–17.5 (Fig. 5A and B and data not shown), which has not been previously reported. We counted 12 serial sections of center region of each kidney ($n=4$ kidneys) and quantified the number of glomeruli. Compared with the control, number of mutant glomeruli was reduced to ~63.2% of that in heterozygous littermate controls at E16.0–16.5 (Fig. 5C). By E17.5, the number of glomeruli in the mutant was further reduced to ~43% of that in heterozygous littermate controls (Fig. 5C). Among all scored mutant glomeruli, ~51.7% displayed obvious dilation of glomerular capillary loops at both stages (Fig. 5C). This suggests that *Tbx18* plays a role in glomerular vascularization.

To further examine the requirement of *Tbx18* in the formation of renal vasculature network, we performed ink injection via renal vein and found that the development of the whole renal vascular network including microvasculature was affected in the mutant. As shown in Fig. 5, the entire vasculature density was largely decreased from as early as E13.5 in all homozygous mutants examined ($n=6$ kidneys for each stage), especially in the

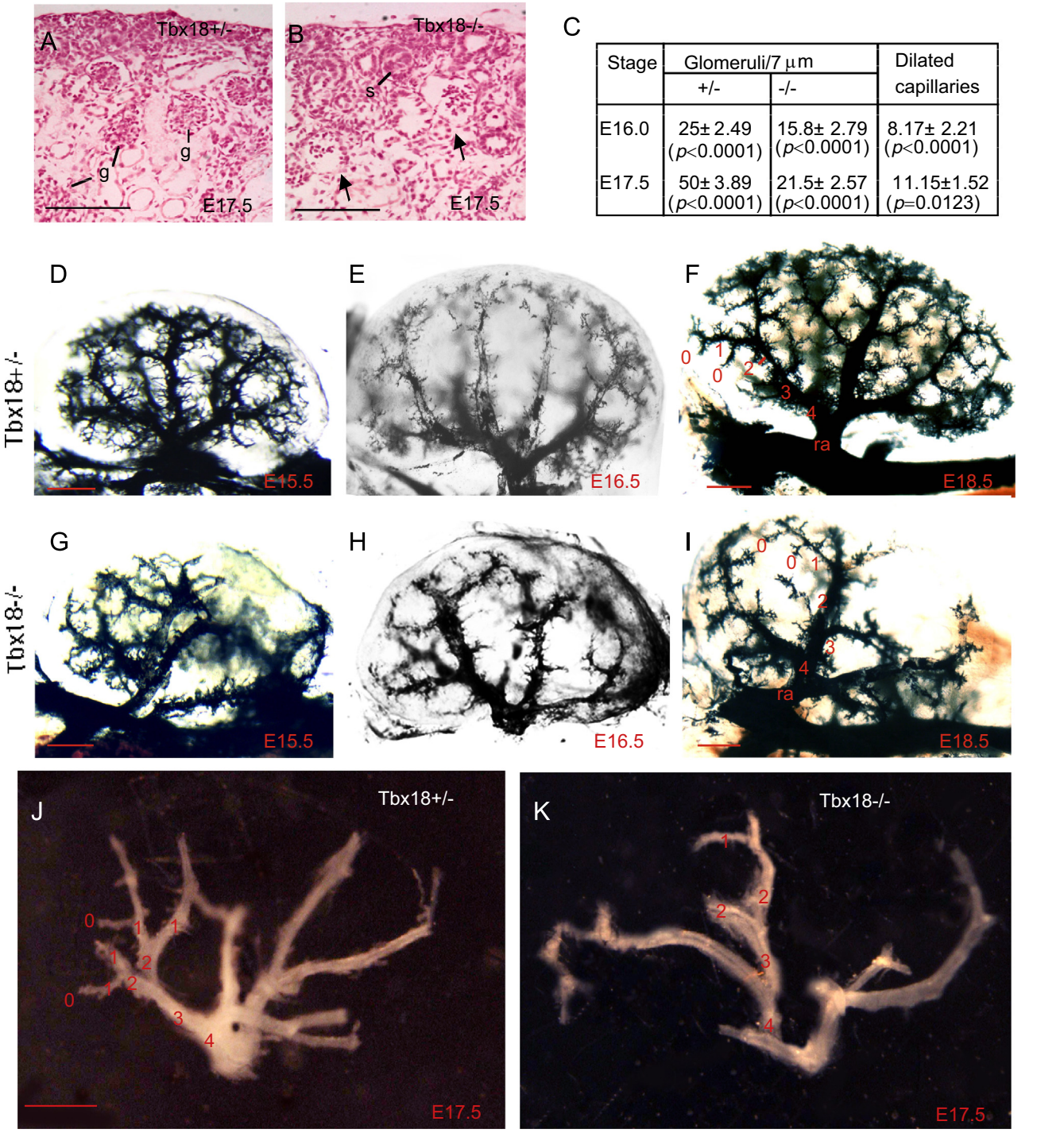


| Stage | Glomeruli/7 μm | | Dilated capillaries |
|---|---|---|---|
| | +/- | -/- | |
| E16.0 | 25± 2.49 ($p$<0.0001) | 15.8± 2.79 ($p$<0.0001) | 8.17± 2.21 ($p$<0.0001) |
| E17.5 | 50± 3.89 ($p$<0.0001) | 21.5± 2.57 ($p$<0.0001) | 11.15±1.52 ($p$=0.0123) |

**Fig. 5.** Perturbation of renal vasculature network in *Tbx18*$^{-/-}$ mice. (A and B) Histological section showing maturing glomeruli (g) in *Tbx18*$^{+/-}$ control and *Tbx18*$^{-/-}$ mutant at E17.5. Arrows point to dilation of capillaries in the mutant glomeruli. (C) Statistic analysis of glomeruli in control and mutant littermates. 12 sections (one out of each 5 serial sections at a thickness of 7 μm) of center region of each kidney ($n$=4 kidneys) were counted separately and the number of glomeruli was quantified. Among all scored mutant glomeruli, dilated glomerular capillary loops were counted and quantified. *P*-values were calculated using the StatView *t*-test; error bars indicate s.d. (D–I) Ink injections for kidney vessels at E15.5, E16.5 and E18.5 and (J and K) microdissected entire intrarenal vasculature of *Tbx18*$^{+/-}$ and *Tbx18*$^{-/-}$ kidneys at E17.5. Terminal vessels are designated as zero-order vessel and the upstreaming vessels are ordered accordingly. Scale bar: 50 μm for A and B and 25 μm for C–H.

posterior region where pelvis was malpositioned (Fig. 5D–I and data not shown). Our gross examination of ink-injected kidneys revealed that although variable between different animals, the renal artery in *Tbx18*$^{-/-}$ kidneys divided irregularly and each segmental artery had fewer branches arising from it (Fig. 5G–I). Furthermore, the vascular arcade in the cortex–medulla junction was poorly formed in the homozygous mutants comparing to the heterozygous animals (Fig. 5E–I). The microdissected entire arterial tree of E17.5 kidneys confirmed these phenotypes (Fig. 5J and K). The entire intrarenal vasculature in the homozygous mutant was also slightly dilated and fragile likely due to loss of vascular SMCs, which was confirmed by SMA, *SM22* and SMHC staining (Fig. 9). Thus, *Tbx18* is necessary for normal development of the whole renal vascular network and glomerular tuft.

*Perturbed development of vascular mesenchyme and glomerular mesangium in Tbx18$^{-/-}$ kidney*

Given that *Tbx18* is expressed in the perivascular mesenchyme and mesangial cells and that the development of vasculature network and glomerular tuft was severely affected in *Tbx18*$^{-/-}$ mice from earlier stages, we focused our analysis on vascular development, especially glomerular vascularization, in the mutant kidney to determine if *Tbx18* plays a direct role in regulating renal vascularization. We first investigated the development of glomerular mesangial cells in *Tbx18*$^{-/-}$ kidney from E15.5 to 16.0, before the onset of ureteric obstruction that occurs from E16.5 (Airik et al., 2006). In *Tbx18*$^{-/-}$ embryos at E16.0, PDGFRβ expression was detectable in the perivascular mesenchymal cells surrounding interlobular arteries and glomerular afferent and efferent arterioles when compared to wild-type controls (Fig. 6A–C, and A′–C′). PDGFRβ+ cells were also present in association with the early stages of glomerulogenesis in the mutant (Fig. 6B–B″), but were fewer than in controls and were mainly located at the juxtaglomerular or at the base area. Very few PDGFRβ+ cells were observed between the expanded capillary loops in the mutants (Fig. 6B, B′, C, and C′, compare with A and A′). As the glomerulus developed further, dilation of capillary loops for the mutant glomeruli became apparent (Fig. 6B–B″, and C–C″). Consistent with the earlier quantification data (Fig. 5C), ~51.5% of all scored mutant glomeruli ($n$=4 kidneys) displayed dilation of glomerular capillary loops.

To rule out the possibility that the abnormal development of glomerular mesangium observed in *Tbx18*$^{-/-}$ mice is a secondary defect caused by the initial build up of urine within the kidney between E15.5 and E16.5 due to obstruction, we dissected kidneys from control and *Tbx18*$^{-/-}$ littermate embryos from E12.5 and cultured in vitro for 4 days (Fig. 7). The growth of kidneys was monitored daily and the mutant kidney appeared noticeably smaller from 1 day in vitro (DIV) when compared with the controls (Fig. 7A and B). Consistent with our earlier observation (Fig. 6), only very few PDGFRβ+ cells were observed at the base area of glomerulus in the mutant kidney explants at 4 DIV (Fig. 7D) when compared to that in wild-type controls (Fig. 7C) and ~50% of all scored mutant glomeruli ($n$=5 kidneys) displayed dilation of glomerular capillary loops (arrowhead, Fig. 7D). Thus, these results identify a primary requirement of *Tbx18* for the development of glomerular mesangial cells.

In addition to the developing glomerulus, the mutant renal capsule displayed decreased PDGFRβ expression compared to controls (red arrowheads, Fig. 7C and D) but elevated PECAM+ cells, which are endothelial cells that are normally localized to the interior of the kidney at E16.5 (green, Fig. 7C and D). Similar observation was obtained in the mutant kidneys at E16.5–17.5 (data not shown). This result suggests that *Tbx18* is also necessary for the formation of the kidney capsule.

At E16.0–16.5, SMA antibody strongly labeled renal arteric and arteriolar walls (Fig. 8A) and weakly the mesangial cells in the maturing glomerulus (Fig. 8B), in contrast to the PDGFRβ expression. In *Tbx18*$^{-/-}$ kidney, detectable SMA-labeled renal arteric and arteriolar walls were much less in the cortex (Fig. 8C), which is likely due to reduction of vasculature density as revealed by ink injection (Fig. 5). SMA+ cells were detectable in some capillary loop renal corpuscles in the mutant but were much weaker, abnormally distributed and often located at the base area

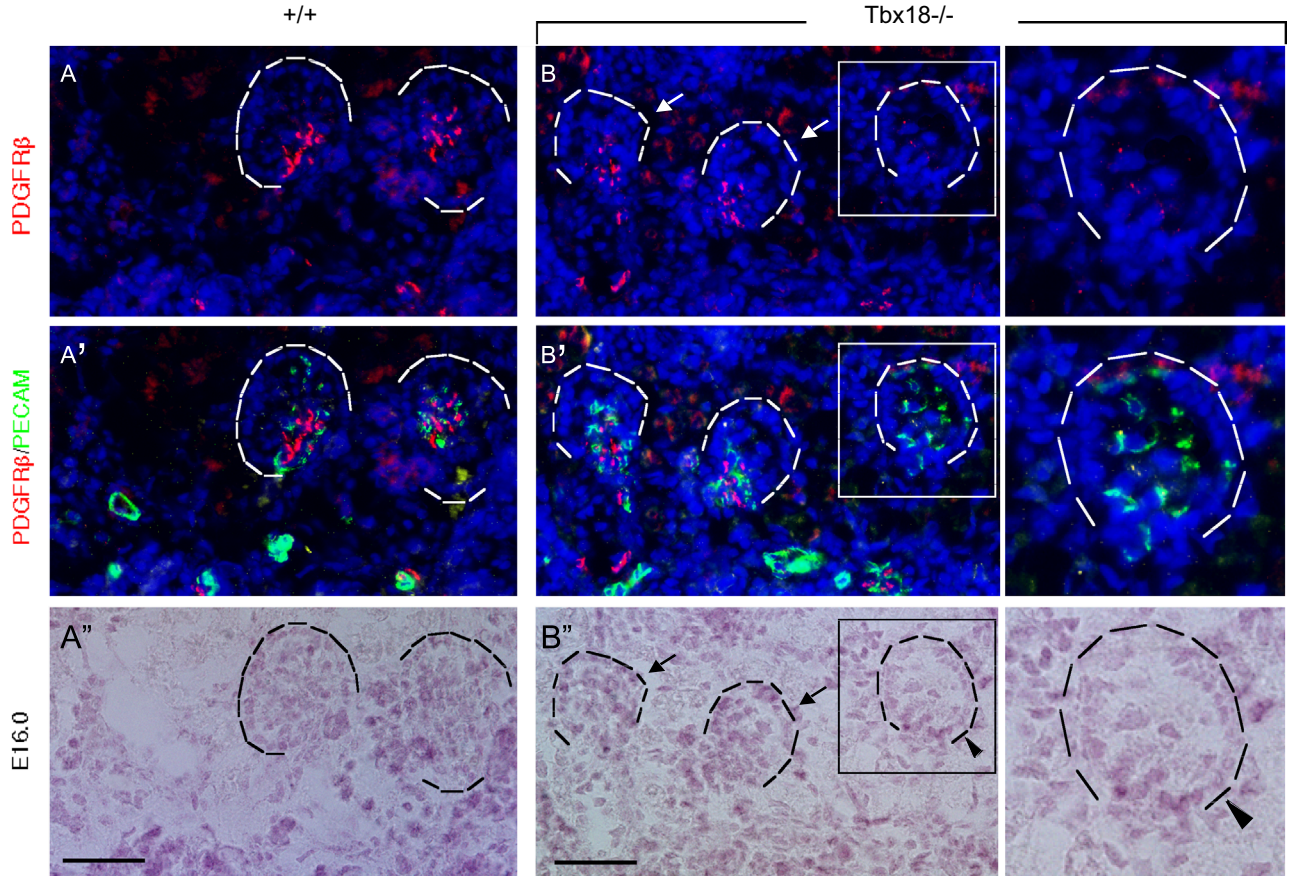


**Fig. 6.** Mesangial cell development is disrupted in *Tbx18*$^{-/-}$ kidney. (A–C′) Co-immunostaining with PDGFRβ (red) and PECAM-1 (green) on kidney sections of *Tbx18*$^{+/-}$ (A and A′) and *Tbx18*$^{-/-}$ (B, B, C, and C′) embryos at E16.0. (A–C″) Bright-filed images of (A–C). Arrows point to earlier cup-shaped glomeruli and arrowheads point to dilated capillaries at late cup-shaped stage in the mutant. Scale bar: 25 μm.

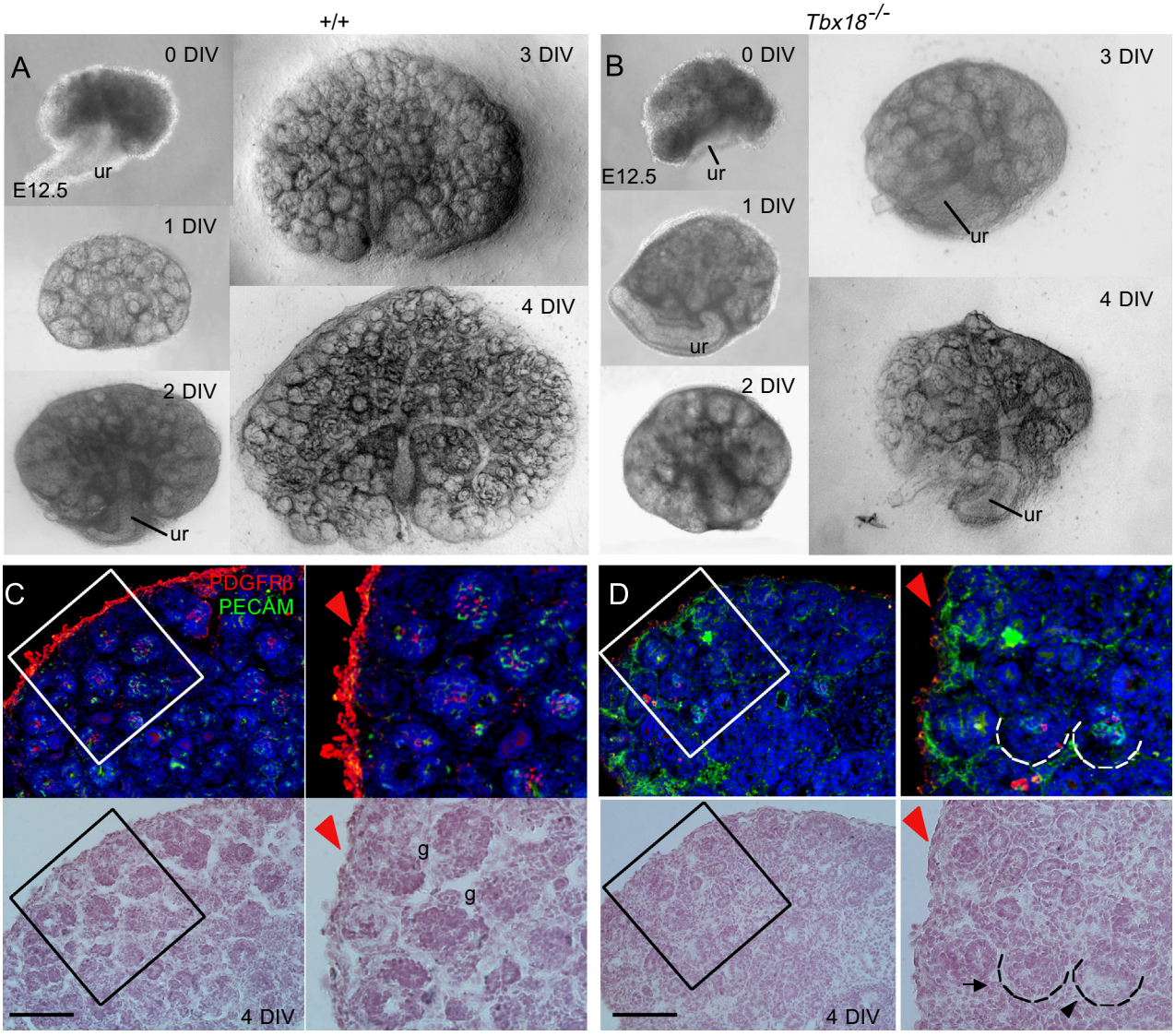


**Fig. 7.** Abnormal development of glomerular mesangium in *Tbx18*$^{-/-}$ kidney explants. (A and B) Bright-field analysis of metanephric explants from E12.5 wild-type and *Tbx18*$^{-/-}$ embryos at 0, 1, 2, 3 and 4 days in vitro (DIV). (C and D) Co-immunostaining with PDGFRβ (red) and PECAM-1 (green). Arrow points to earlier cup-shaped glomerulus and black arrowhead points to dilated capillary at late maturation stage in the mutant. Red arrowhead points to increased PECAM+ cells but decreased PDGFRβ expression in the mutant renal capsule (D) when compared to the wild-type controls (C). Right panels are higher magnification of the boxed areas in C and D. Scale bar: 50 μm.

(Fig. 8D). In addition, SMA expression was weaker in the renal capsule (red arrow, Fig. 8C) and the cortex in the mutant kidney when compared to wild-type control (Fig. 8A), whereas PECAM expression was elevated in the mutant renal capsule (red arrow, Fig. 8C′, compare to A′). These data further indicate that *Tbx18* is necessary for normal development of glomerular mesangial cells as well as renal capsule formation.

Whole-mount SMA staining confirmed reduction of vasculature density and disorganization of SMCs in *Tbx18*$^{-/-}$ kidneys at E17.5 (Fig. 9A and B). The number of SMA+ cells surrounding the vessels in the kidney was also markedly decreased in *Tbx18*$^{-/-}$ kidneys when compared with heterozygous controls (Fig. 9C and D and data not shown). Similar observation was obtained with *SM22* (smooth muscle-specific gene) riboprobe and smooth muscle heavy chain (SMHC) antibody staining at later stages (Fig. 9E–H). SMA and SMHC antibody staining also revealed disorganization and aberrant distribution of SMCs in the pelvic region of *Tbx18*$^{-/-}$ kidneys at E16.5–P0 (Fig. 9D and H and data not shown). Thus, *Tbx18* is required for smooth muscle formation of renal vessels.

### *Reduced cell proliferation in glomerular mesangium and increased apoptosis in vascular mesenchyme in Tbx18*$^{-/-}$ *kidney*

We performed immunofluoresence staining using anti-PCNA, a marker for proliferating cell nuclei, during kidney development by focusing on the cup-shaped vesicles at which glomerular development begins to fail in the mutant. In wild-type cup-shaped vesicles, PCNA+ cells were detected in central part of the mesenchymal core, which contains mesangial progenitors, and in the periphery where endothelial cells are located (Fig. 10A and B). In *Tbx18*$^{-/-}$ kidneys, fewer cells in the mesenchymal core were positive for PCNA (Fig. 10B). Following ballooning of the capillaries during glomerular maturation in the mutant, few PCNA+ cells in the mesenchymal core were detected (Fig. 10D). Since PDGFRβ+ cells were located in the juxtaglomerular area or at the base area in the mutant glomerulus, the PCNA+ cells observed in the mutant glomerulus could be proliferating endothelial cells. BrdU-incorporation assay confirmed that there were fewer cycling cells in the mesenchymal core in the mutant glomerulus (Fig. 10F,

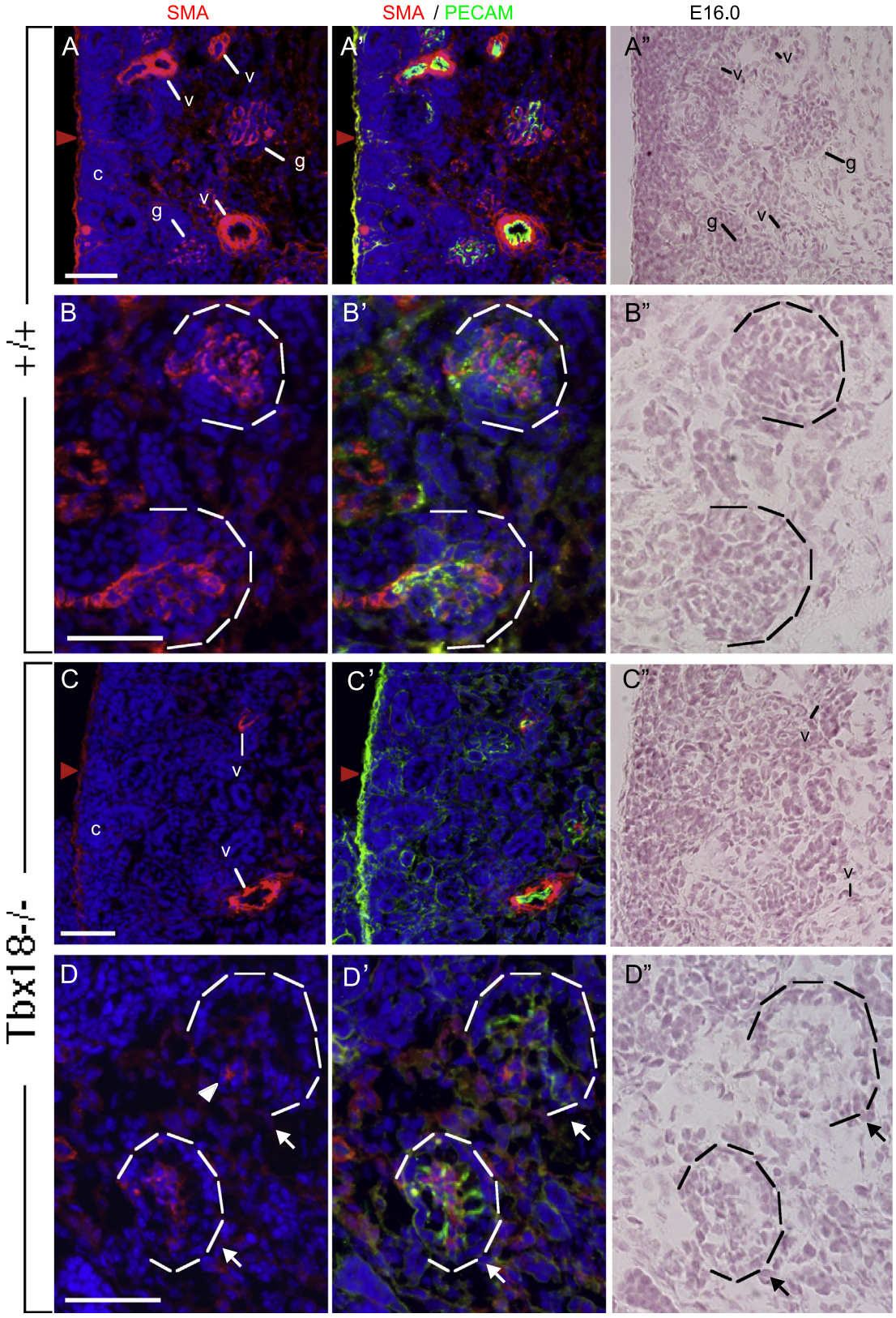


**Fig. 8.** Perturbed vasculature and glomerular tuft development in *Tbx18*$^{-/-}$ kidney. (A–D and A′–D′) Kidney sections immunostained with anti-SMA and -PECAM-1 showing strong SMA+ cells in vascular system in cortex and medulla next to cortex (A, A′, C, and C′) and weak staining in late cup-shaped glomeruli (B, B′, D, and D′) of wild-type (A, A′, B, and B′) and *Tbx18*$^{-/-}$ embryos (C, C′, D, and D′) at E16.0. (A″–D″) Bright-filed images of (A–D). Arrow points point to capillary dilation in the mutant. Scale bar: 25 μm.

compare with E). We counted 15 maturing glomeruli and quantified the proliferating nuclei. While the proliferation rate in the endothelial layer appeared to be increased in the mutant compared to the wild-type control ($0.56 \pm 0.07$ versus $0.31 \pm 0.06$ per glomerulus), the proliferation rate in the mesenchymal core was markedly decreased in the mutant ($0.06 \pm 0.04$ versus $0.43 \pm 0.08$

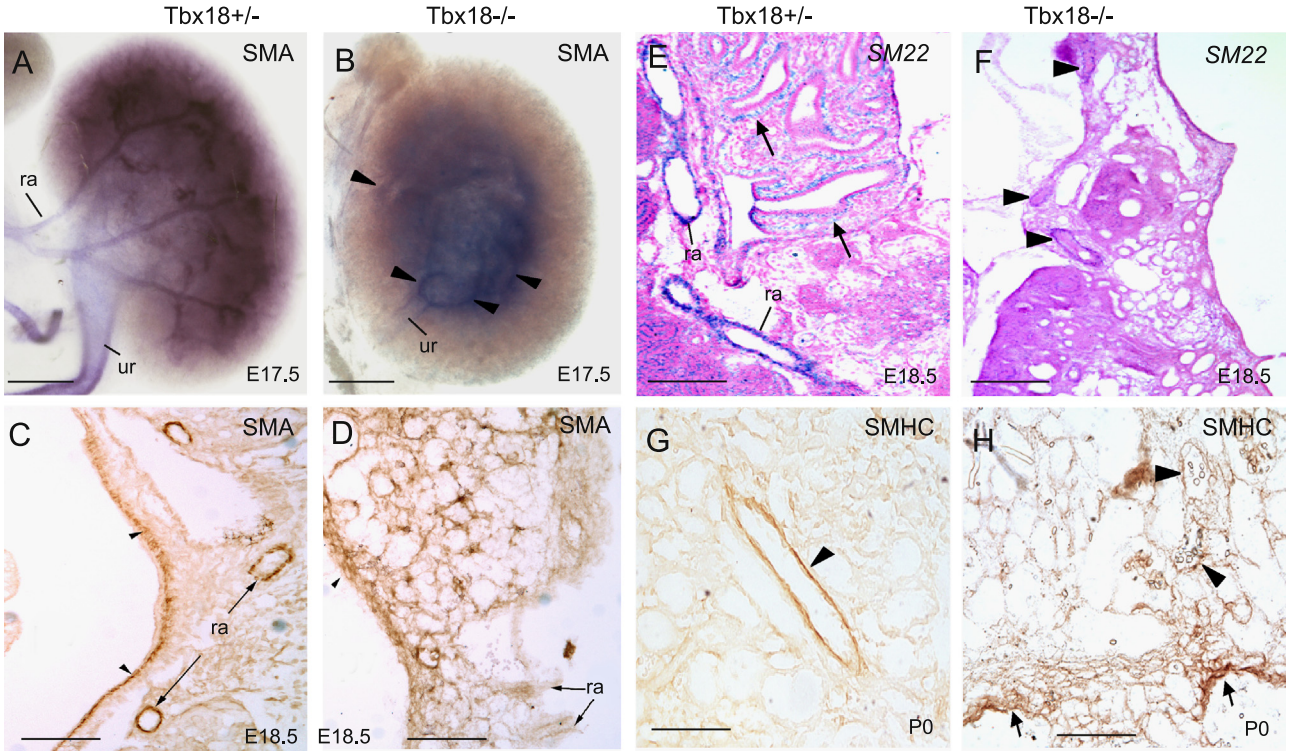


**Fig. 9.** Defective development of SMCs in *Tbx18*$^{-/-}$ kidney. (A and B) Whole-mount immunostaining for α-SMA in E17.5 kidneys showing reduced α-SMA expression in a *Tbx18*$^{-/-}$ artery branch (arrowheads). (C and D) Immunostaining for αSMA on E18.5 kidney sections. SMA+ cells are largely reduced in vascular system and pelvic region (arrowheads). (E and F) Section in situ hybridization for *SM22* at E18.5. Arrows (E) point to SMCs in the pelvic region. Arrowheads (F) point to reduced *SM22* expression in the mutant renal arteries. (G and H) Immunostaining for smooth muscle heavy chains (SMHC) on P0 kidney sections. Arrowheads point to renal vessels and arrows in H point to disorganized and aberrant distribution of SMCs in the pelvic region in *Tbx18*$^{-/-}$ kidneys. pv, renal pelvis; ra, renal artery; ur, ureter. Scale bar: 25 μm.

in control) (Fig. 10G). However, overall proliferation rate in both cell types (endothelial and mesenchymal) was only slightly reduced in the mutant ($0.35 \pm 0.05$) when compared with wild-type control ($0.39 \pm 0.09$). Nonetheless, our result suggests that reduced proliferation may contribute to reduced cell numbers in the mesenchymal core in the mutant glomerulus.

We next examined apoptosis by TUNNEL assay. By E15.5, apoptotic cells were widespread vascular mesenchyme (Fig. 10J, compared with I), pre-cystic epithelia and their surrounding mesenchyme (Fig. 10N, compare with M) as well as in the renal capsule (Fig. 10P, compare with O) in the mutant. We counted apoptotic cells from 20 transverse sections of blood vessels and found that abnormal cell death in the vascular mesenchyme as well as in endothelial layer of *Tbx18*$^{-/-}$ embryos was increased (Fig. 10H). In contrast, increased cell death was not observed in the developing glomerulus (Fig. 10H–L), although apoptotic cells were increased in the juxtaglomerular or the base area of the mutant glomerulus (Fig. 10L). These results indicate that cell survival was an early cellular defect that leads to failure of vasculature development in *Tbx18*$^{-/-}$ mice.

## Discussion

Previous studies provided substantial evidence that the development of ureteral mesenchyme depends on *Tbx18* function (Airik et al., 2006; Bohnenpoll et al., 2013; Nie et al.), but did not address if *Tbx18* has a primary role in kidney development, and kidney defects observed in the mutant were suggested to be secondary due to ureteric obstruction (Airik et al., 2006). Moreover, it was still unknown whether *Tbx18* is expressed in the developing kidney. The present work supports a primary role for *Tbx18* in renal vasculature network based on the following evidence. First, *Tbx*18 is endogenously expressed in renal vasculture and glomerular mesangium and *Tbx18*-derived cells directly participate in renal vessel and glomerular mesangium development. Second, abnormal renal vascularization, including altered vessel arrangement, reduced vascular density and dilation of glomerular capillaries, can be detected in the mutant at early stages before the onset of ureteric obstruction and in kidney explants cultured from E12.5.

### *The multiple mesenchymal population of Tbx18+ cells in the kidney are stromal cells*

Our genetic cell fate analysis revealed that *Tbx18+* progenitors directly contribute to glomerular mesangium, vascular SMCs and pericytes, and renal interstitial cells, which form supporting tissues for endothelia and epithelia. The multiple mesenchymal cell populations derived from *Tbx18+* cells are stromal cells, which originate from *Foxd1+* precursors in the periphery of the MM (Faa et al., 2012; Humphreys et al., 2010; Sequeira Lopez and Gomez, 2011). No contribution is seen to other structures of the kidney and no evidence is observed for an ongoing recruitment of this mesenchymal population to the ureteric epithelium or tubular epithelia.

Our result is in general agreement with cell fate studies using *Foxd1*$^{Cre}$ mice (Humphreys et al., 2010). Both genes show overlapping expression pattern in the renal capsule (Levinson et al., 2005). However unlike *Foxd1*, *Tbx18* is not expressed in the cortical stroma at E11.5–12.5, when *Foxd1* has already been activated (Bohnenpoll et al., 2013; Hatini et al., 1996; Levinson et al., 2005), and weak *Tbx18* expression in cortical stroma becomes detectable after E12.5 (Figs. 1 and S1). Once *Tbx18* is turned on in the cortical stromal cells at later stages, *Tbx18+* cells substantially overlap with *Foxd1+* cells. Our lineage tracing at

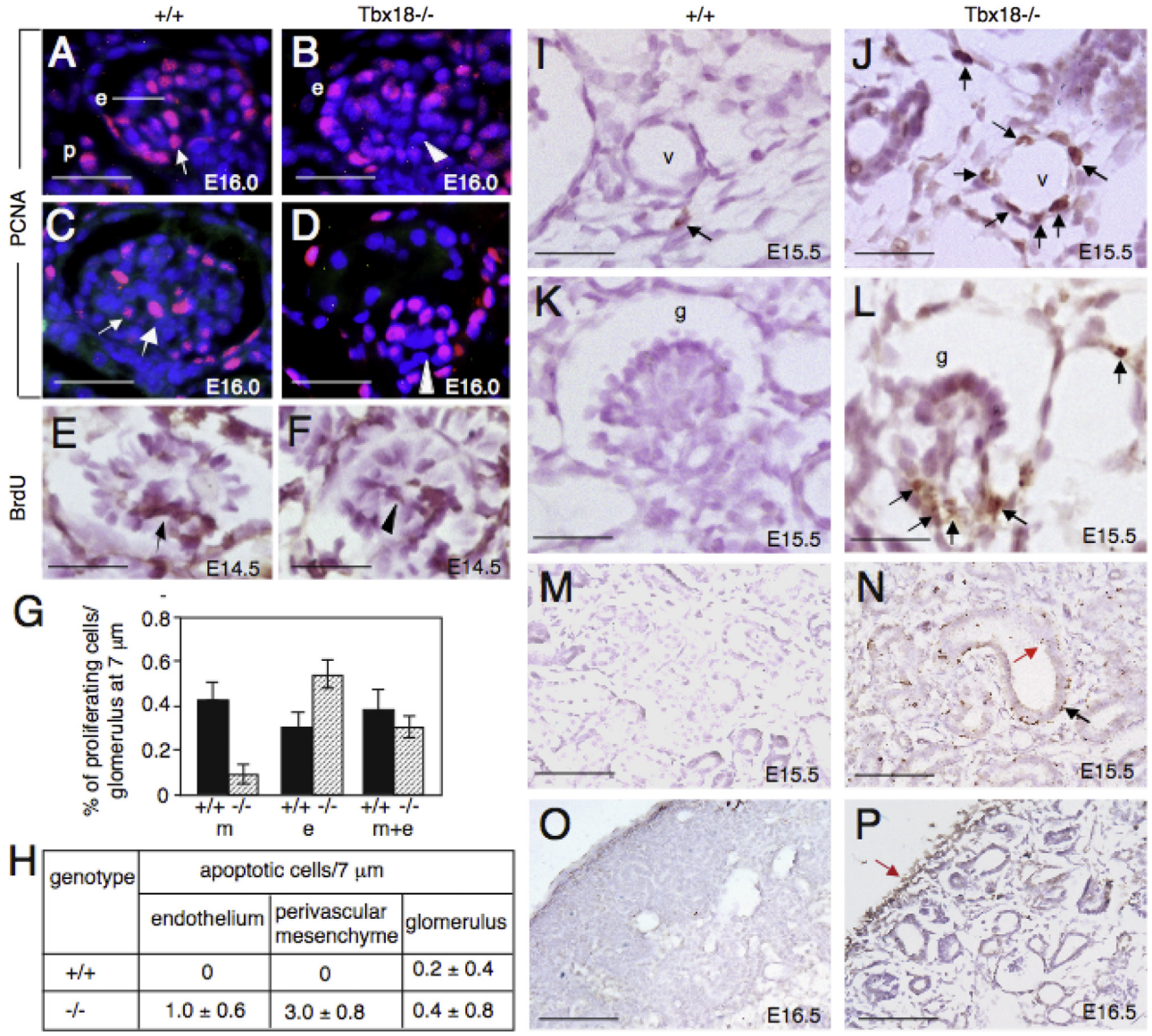


**Fig. 10.** Proliferation and apoptosis in *Tbx18*$^{-/-}$ kidneys. (A–D) Immunostaining with anti-PCNA antibody showing proliferating cells in mesangial core in control (arrows) and reduced proliferating mesangial cells in the mutant (arrowheads) at E16.0. (E and F) BrdU-labeling showing BrdU-positive cells in the center of mesangial core in control (arrow) and reduced BrdU-positive in the mutant (arrowhead) at E14.5. (G) Statistical analysis of PCNA+ cells in mesangial cells, endothelial cells or both cell types between the mutant and control. In the mesangial cells (m) $P=0.1461$ ($0.43 \pm 0.08$) in control versus $P=0.0425$ ($0.06 \pm 0.04$) in mutant. In the endothelial cells (e) $P=0.2927$ ($0.31 \pm 0.06$) in control versus $P=0.3364$ ($0.56 \pm 0.07$) in mutant. In both cell types (m+e) $P=0.2761$ ($0.39 \pm 0.09$) in control versus $P=0.1673$ ($0.35 \pm 0.05$) in mutant. *P*-values were calculated using the StatView *t*-test; error bars indicate s.d. (H) TUNEL-positive cells (brown nuclei) were counted from 10 glomeruli or 10 serial transverse sections of blood vessels on serial sections (from at least six vessels). Shown are the average number of TUNEL-positive cells per section (10 μm) for each genotype for vessels or for each glomerulus (10 μm). (I–P) TUNNEL assay on sections of wild-type and *Tbx18*$^{-/-}$ kidneys at E15.5 and E16.5. Arrows point to very few apoptotic cells in control (I) and increased abnormal cell death in the mutant in both endothelium and mesenchyme (J and L), epithelia (red arrow in N) and its surrounding mesenchyme (black arrow in N) and renal capsule (P). Scale bar: 25 μm for A–F and I–L, and 100 μm for M–P.

E11.5–12.5 also excluded the possibility that there might be an early *Tbx18*+ population at E10.5 that might overlap with *Foxd1*+ progenitors and contributes to kidney formation. Thus, strong *Tbx18* expression in the cortical stroma is likely induced after E12.5 and *Tbx18*+ cortical stromal cells are most likely to be hierarchically downstream of *Foxd1*+ cells.

Consistent with the idea that *Foxd1* is upstream of *Tbx18* in the stromal cells, its expression in *Tbx18*$^{-/-}$ kidney is virtually normal at E12.5 (Airik et al., 2006). Since the onset of *Foxd1* appears to occur earlier than that of *Tbx18*, *Foxd1* might have an unique early role in cortical stromal cells. This would explain why the *Foxd1*$^{-/-}$ kidneys are not detached from the dorsal body wall (Levinson et al., 2005), which was not observed in *Tbx18*$^{-/-}$ animals. Interestingly, however, *Foxd1*$^{-/-}$ mice had kidney defects similar in many ways to *Tbx18*$^{-/-}$ mice, i.e. pelvic kidney and failure of medial rotation (Levinson et al., 2005), providing further support that *Tbx18* is a stromal cell regulator during kidney development. One intriguing phenotype shared by these two mutant mice is the malformed renal capsule with increased PECAM+ cells. In the *Foxd1* mutant kidney capsule, not only increased PECAM+ cells but also ectopic Bmp4+ cells are observed (Levinson et al., 2005). This ectopic Bmp4 signaling in the renal capsule in *Foxd1* mutant kidneys has been shown to indirectly cause multiple number of pre-tubular aggregates/UB ampulla at earlier stages, resulting in patterning defects of the ureteric tree as well as a delay in the nephrogenesis in the mutant before E16.5 (Levinson et al., 2005). In *Tbx18*$^{-/-}$ kidneys, decreased PDGFRβ expression in the capsule was also observed (Fig. 7), further suggesting that the mutant

kidney capsule is malformed. Although our marker analysis at E13.5–17.5 indicated that the nephron differentiation in *Tbx18*$^{-/-}$ kidneys is not blocked, we speculate that the malformed renal capsule may contribute to patterning defects in ureteric branching and/or nephrogenesis. Detailed analysis regarding the cellular and molecular basis for the observed capsule defects in *Tbx18*$^{-/-}$ kidneys and whether these defects contribute to the patterning defects of the ureteric colleting system and nephrogenesis at different embryonic stages are underway in our laboratory. Furthermore, since *Foxd1* is not expressed in the ureteral mesenchyme-derived SMCs in the ureter and pelvic region, *Foxd1*$^{Cre}$ should serve as a better deletor to conditionally remove *Tbx18* in the kidney *Foxd1*+ stromal cells. Nonetheless, the overlapping expression patterns of these two genes and the similarities of the phenotype observed in their mutant kidneys suggest that these two genes may act in a same regulatory pathway to mediate renal stromal cell development. Future studies are required to examine their potential interaction in the kidney.

*The role of Tbx18 in vascular development*

A key defect observed in *Tbx18*$^{-/-}$ kidney is the disruption of vasculature formation. Endothelial cells of renal vasculature arise from both renal blastema vasculogenesis and angiogenesis from existing renal arteries and veins (Del Porto et al., 1999; Gomez et al., 1997; Oliver and Al-Awqati, 2000; Oliver et al., 2002; Risau and Ekblom, 1986; Risau et al., 1988), whereas their associated SMCs and pericytes and mesangial cells are derived from *Foxd1*-derived stromal cells (Humphreys et al., 2010; Kida and Duffield, 2011; Sequeira Lopez and Gomez, 2011). Normal expression of *Foxd1* in *Tbx18*$^{-/-}$ kidneys at E12.5 suggests that the initial development of the stromal cells is not affected. Detectable expression of molecular markers downstream of *Foxd1*, including α-SMA, *SM22*, SMHC and PDGFRβ, in *Tbx18*$^{-/-}$ kidney also indicates that *Tbx18* is not required for cell fate specification of the stromal cells-derived vascular mesenchymal cells and mesangial cells. However, as the wall of kidney vessels was apparently abnormal with reduced or incomplete smooth muscle tissue as indicated by altered PDGFRβ, α-SMA, *SM22* and SMHC staining, *Tbx18* is clearly necessary for proper differentiation of stromal cells. One possible action for *Tbx18* in mediating stromal cell differentiation is regulating cell survival. In the absence of *Tbx18*, the differentiating SMCs undertake the cell death pathway, as detected by the TUNEL assay.

Our results reveal a novel function of *Tbx18* in glomerular tuft development. The sudden ballooning of the glomerular capillary loops at maturation stages may suggest a failure of mesangial cells to make focal attachments to the glomerular basement membrane, which separates the endothelial and mesangial cells from the urinary space. Glomerular capillaries develop by angiogenic sprouting from the afferent/efferent arteriole and it is believed that mesangial cells in this process are co-recruited from PDGFRβ+ arteriolar SMC progenitors at the juxtaglomerular area involving proliferation and migration of both endothelial and mesangial cells (Hugo et al., 1997; Lindahl et al., 1997, 1998). Since PDGFRβ expression is markedly reduced in *Tbx18*$^{-/-}$ mutant kidneys such as the renal capsule and mesangial and other stromal cells, *Tbx18* may be involved in the regulation of PDGFRβ expression to mediate mesangium and stromal cell development. The presence of fewer PDGFRβ+ cells detected in *Tbx18*$^{-/-}$ mutants at juxtaglomerular perivascular sites or at the base area in early stages of glomerular development suggests a defect in recruitment of mesangial progenitors in the course of glomerular maturation. Although we cannot exclude the possibility that there may be a defect in cell migration, as some PDGFRβ+ cells do enter the vesicle, we speculate that the impairment may involve a defect in the ability of these cells to proliferate or survive once they have entered the vesicle. Reduced proliferation would explain why the number of cells is smaller in this structure in the mutant. Indeed, PCNA staining and BrdU-labeling revealed that fewer cells were proliferating in the mesangium core and the mitotic index was decreased (Fig. 10). Thus, *Tbx18* may have a role in regulating mesangial cell proliferation during glomerular maturation and the sudden ballooning of the glomerular capillary loops in the mutant could be caused by lack of cells. It is also possible that there is a defect in cell differentiation or function such as extracellular matrix synthesis and secretion. Studies are underway in our laboratory to examine these possibilities.

Although TUNEL staining failed to detect increased apoptosis in the developing mesangium of mutant glomeruli, increased cell death was detected in the perivascular mesenchyme at the base or juxtaglomerular area, indicating that the loss of mesangial cells could be at least in part attributed to increased cell death.

In addition to the defects in the mesenchyme that are directly associated with the epithelia or endothelia, the interstitium in *Tbx18*$^{-/-}$ kidneys is poorly formed. Phenotypic and marker analysis indicated disorganization and defective differentiation of interstitial cells in the mutant (Fig. 4 and data not shown). Such defects are likely to affect ECM formation, which is critical to maintain structural integrity in the developing kidney. This is particularly obvious in the medulla, but also occurs in the cortex. As expected, collecting ducts and nephron tubule dilation was not only found in the medulla but also in the cortex from ~E16.5 by lectin staining (Fig. 4C and D and data not shown). However, tissue-specific knockout is necessary to rule out the possibility that these defects could be secondary due to initial urine accumulation in the mutant kidney. Nonetheless, overall, malformation of kidney stromal compartments serves as the primary cause of abnormal kidney development in *Tbx18*$^{-/-}$ mice. As no *Tbx18*+ cells contribute to endothelial or epithelial structures in the kidney, defects seen in *Tbx18*$^{-/-}$ kidney epithelia or endothelia are likely to be secondary due to the malformation of their surrounding mesenchymal supporting tissues. This work not only supports the earlier studies (Airik et al., 2006; Bohnenpoll et al., 2013), but also reveals novel roles of *Tbx18* in the mesenchymal cell populations during kidney development.

## Acknowledgments

We thank J. Li for the technical assistance. This work was supported by NIH RO1 DK064640 (P.-X.X).

## Appendix A. Supporting information

Supplementary data associated with this article can be found in the online version at http://dx.doi.org/10.1016/j.ydbio.2014.04.006.

## References

Abrahamson, D.R., Robert, B., Hyink St, D.P., John, P.L., Daniel, T.O., 1998. Origins and formation of microvasculature in the developing kidney. Kidney Int. Suppl. 67, S7–S11.

Airik, R., Bussen, M., Singh, M.K., Petry, M., Kispert, A., 2006. Tbx18 regulates the development of the ureteral mesenchyme. J. Clin. Investig. 116, 663–674.

Alcorn, D., Maric, C., McCausland, J., 1999. Development of the renal interstitium. Pediatr. Nephrol. 13, 347–354.

Batourina, E., Gim, S., Bello, N., Shy, M., Clagett-Dame, M., Srinivas, S., Costantini, F., Mendelsohn, C., 2001. Vitamin A controls epithelial/mesenchymal interactions through Ret expression. Nat. Genet. 27, 74–78.

Bohnenpoll, T., Bettenhausen, E., Weiss, A.C., Foik, A.B., Trowe, M.O., Blank, P., Airik, R., Kispert, A., 2013. Tbx18 expression demarcates multipotent precursor populations in the developing urogenital system but is exclusively required

within the ureteric mesenchymal lineage to suppress a renal stromal fate. Dev. Biol. 380, 25–36.
Bussen, M., Petry, M., Schuster-Gossler, K., Leitges, M., Gossler, A., Kispert, A., 2004. The T-box transcription factor Tbx18 maintains the separation of anterior and posterior somite compartments. Genes Dev. 18, 1209–1221.
Cai, C.L., Martin, J.C., Sun, Y., Cui, L., Wang, L., Ouyang, K., Yang, L., Bu, L., Liang, X., Zhang, X., Stallcup, W.B., Denton, C.P., McCulloch, A., Chen, J., Evans, S.M., 2008. A myocardial lineage derives from Tbx18 epicardial cells. Nature 454, 104–108.
Casellas, D., Dupont, M., Kaskel, F.J., Inagami, T., Moore, L.C., 1993. Direct visualization of renin-cell distribution in preglomerular vascular trees dissected from rat kidney. Am. J. Physiol. 265, F151–F156.
Cullen-McEwen, L.A., Caruana, G., Bertram, J.F., 2005. The where, what and why of the developing renal stroma. Nephron Exp. Nephrol. 99, e1–e8.
Del Porto, F., Mariotti, A., Ilardi, M., Messina, F.R., Afeltra, A., Amoroso, A., 1999. Kidney vasculogenesis and angiogenesis: role of vascular endothelial growth factor. Eur. Rev. Med. Pharmacol. Sci. 3, 149–153.
Dressler, G.R., 2006. The cellular basis of kidney development. Annu. Rev. Cell Dev. Biol. 22, 509–529.
Faa, G., Gerosa, C., Fanni, D., Monga, G., Zaffanello, M., Van Eyken, P., Fanos, V., 2012. Morphogenesis and molecular mechanisms involved in human kidney development. J. Cell. Physiol. 227, 1257–1268.
Farin, H.F., Mansouri, A., Petry, M., Kispert, A., 2008. T-box protein Tbx18 interacts with the paired box protein Pax3 in the development of the paraxial mesoderm. J. Biol. Chem. 283, 25372–25380.
Gomez, R.A., Norwood, V.F., Tufro-McReddie, A., 1997. Development of the kidney vasculature. Microsc. Res. Tech. 39, 254–260.
Hatini, V., Huh, S.O., Herzlinger, D., Soares, V.C., Lai, E., 1996. Essential role of stromal mesenchyme in kidney morphogenesis revealed by targeted disruption of Winged Helix transcription factor BF-2. Genes Dev. 10, 1467–1478.
Hugo, C., Shankland, S.J., Bowen-Pope, D.F., Couser, W.G., Johnson, R.J., 1997. Extraglomerular origin of the mesangial cell after injury. A new role of the juxtaglomerular apparatus. J. Clin. Investig. 100, 786–794.
Humphreys, B.D., Lin, S.L., Kobayashi, A., Hudson, T.E., Nowlin, B.T., Bonventre, J.V., Valerius, M.T., McMahon, A.P., Duffield, J.S., 2010. Fate tracing reveals the pericyte and not epithelial origin of myofibroblasts in kidney fibrosis. Am. J. Pathol. 176, 85–97.
Kida, Y., Duffield, J.S., 2011. Pivotal role of pericytes in kidney fibrosis. Clin. Exp. Pharmacol. Physiol. 38, 467–473.
Kloth, S., Aigner, J., Schmidbauer, A., Minuth, W.W., 1994. Interrelationship of renal vascular development and nephrogenesis. Cell Tissue Res. 277, 247–257.
Levinson, R.S., Batourina, E., Choi, C., Vorontchikhina, M., Kitajewski, J., Mendelsohn, C.L., 2005. Foxd1-dependent signals control cellularity in the renal capsule, a structure required for normal renal development. Development 132, 529–539.
Lindahl, P., Hellstrom, M., Kalen, M., Karlsson, L., Pekny, M., Pekna, M., Soriano, P., Betsholtz, C., 1998. Paracrine PDGF-B/PDGF-Rbeta signaling controls mesangial cell development in kidney glomeruli. Development 125, 3313–3322.
Lindahl, P., Johansson, B.R., Leveen, P., Betsholtz, C., 1997. Pericyte loss and microaneurysm formation in PDGF-B-deficient mice. Science 277, 242–245.
Mendelsohn, C., Batourina, E., Fung, S., Gilbert, T., Dodd, J., 1999. Stromal cells mediate retinoid-dependent functions essential for renal development. Development 126, 1139–1148.
Moffat, D.B., Fourman, J., 2001. A vascular pattern of the rat kidney. 1963. J. Am. Soc. Nephrol. 12, 624–632.
Nie, X., Sun, J., Gordon, R.E., Cai, C.L., Xu, P.X., 2010. SIX1 acts synergistically with TBX18 in mediating ureteral smooth muscle formation. Development. 137, 755–765.
Oliver, J., Al-Awqati, Q., 2000. Development of vascular elements during renal organogenesis. Kidney Int. 57, 2167–2168.
Oliver, J.A., Barasch, J., Yang, J., Herzlinger, D., Al-Awqati, Q., 2002. Metanephric mesenchyme contains embryonic renal stem cells. Am. J. Physiol. Renal Physiol. 283, F799–F809.
Quaggin, S.E., Schwartz, L., Cui, S., Igarashi, P., Deimling, J., Post, M., Rossant, J., 1999. The basic-helix-loop-helix protein pod1 is critically important for kidney and lung organogenesis. Development 126, 5771–5783.
Risau, W., Ekblom, P., 1986. Production of a heparin-binding angiogenesis factor by the embryonic kidney. J. Cell Biol. 103, 1101–1107.
Risau, W., Sariola, H., Zerwes, H.G., Sasse, J., Ekblom, P., Kemler, R., Doetschman, T., 1988. Vasculogenesis and angiogenesis in embryonic-stem-cell-derived embryoid bodies. Development 102, 471–478.
Saxen, L., Sariola, H., 1987. Early organogenesis of the kidney. Pediatr. Nephrol. 1, 385–392.
Saxen, L., Sariola, H., Lehtonen, E., 1986. Sequential cell and tissue interactions governing organogenesis of the kidney. Anat. Embryol. (Berl.) 175, 1–6.
Sequeira Lopez, M.L., Gomez, R.A., 2011. Development of the renal arterioles. J. Am. Soc. Nephrol. 22, 2156–2165.
Soriano, P., 1999. Generalized lacZ expression with the ROSA26 Cre reporter strain. Nat. Genet. 21, 70–71.
Srinivas, S., Goldberg, M.R., Watanabe, T., D'Agati, V., al-Awqati, Q., Costantini, F., 1999. Expression of green fluorescent protein in the ureteric bud of transgenic mice: a new tool for the analysis of ureteric bud morphogenesis. Dev. Genet. 24, 241–251.
Xu, P.X., Zheng, W., Huang, L., Maire, P., Laclef, C., Silvius, D., 2003. Six1 is required for the early organogenesis of mammalian kidney. Development 130, 3085–3094.